2025, VOL:2, ISSUE:1 Pages:2025_2 https://doi.org/10.5281/zenodo.16812153

INTBECM International Bulletin of Electrochemical Methodology

Electrochemical Detection and DNA Interaction of Gilaburu (*Viburnum opulus*) Extract from Commercial Tablets

Hüseyin Oğuzhan KAYA[a], Sena ALACACI [b], Seda Nur TOPKAYA[c,d*]

[a], *İzmir Katip Çelebi University, Faculty of Pharmacy, Department of Analytical Chemistry, Izmir, Türkiye*
[b], *İzmir Katip Çelebi University, Faculty of Pharmacy, Izmir, Türkiye*
[c], *Izmir Biomedicine and Genome Center, Izmir, Türkiye*
[d], *Dokuz Eylul University, Izmir International Biomedicine and Genome Institute, Izmir, Türkiye*

ABSTRACT

Gilaburu *(Viburnum opulus)* is a medicinal plant known for its diverse pharmacological properties, including anticancer, antioxidant, antimicrobial, and vasodilatory effects. Traditionally, it has been used in the treatment of respiratory, gastrointestinal, urogenital, and metabolic disorders In this study, the electroactivity of Gilaburu (Viburnum opulus) extract was detected directly from its commercial tablet form using differential pulse voltammetry (DPV) and cyclic voltammetry (CV), and its interaction with double-stranded DNA (dsDNA) was electrochemically investigated. The interaction between the extract and double-stranded DNA (dsDNA) was investigated in solution phase by monitoring the oxidation peak potentials and currents of guanine and adenine. Following the interaction, a significant decrease in the adenine oxidation peak current and a positive shift in its peak potential were observed, indicating an intercalative binding mode. Based on the reduction in adenine signal, the extract exhibited approximately 65% toxicity toward dsDNA, suggesting a moderate level of DNA damage. The ability to directly detect Gilaburu extract from commercial tablets highlights the practical applicability of this electrochemical approach for pharmaceutical quality control. The method demonstrated high sensitivity, with limits of detection (LOD) and quantification (LOQ) calculated as 4.5 and 15.1 µg/mL, respectively. The results provide an initial framework for understanding the molecular mechanisms underlying the pharmacological activity of Gilaburu through its interactions with nucleic acids.

KEYWORDS
Herbal drug analysis, Gilaburu (*Viburnum opulus*), Electrochemical characterization, Drug-DNA Interaction, Differential Pulse Voltammetry

1. INTRODUCTION

Recent advancements in herbal therapy have been largely driven by growing concerns over the limited success of conventional drug discovery and the increasing challenges related to therapeutic efficacy. Medicinal plants have historically been employed in nearly all regions as traditional treatments for a wide range of diseases and infections, largely due to their therapeutic versatility and minimal side effects [1]. One of these medicinal plants of Gilaburu *(Viburnum opulus*), belonging to the Adoxaceae family, is a widely distributed species with recognized applications in the medicinal, nutritional, and ornamental domains. The genus is native to a broad geographic region extending from South America to

*Contact: Seda Nur TOPKAYA, sedanur6@gmail.com

Southeast Asia and includes over 230 endemic species [2, 3]. Gilaburu has been traditionally used for the management of various health conditions, including respiratory, gastrointestinal, urogenital, metabolic, and neurological disorders. Recent studies have demonstrated that its bioactive constituents can enhance mucosal defense mechanisms and possess notable antimicrobial, antioxidant, anticancer, and vasodilatory activities. The therapeutic potential of Gilaburu is primarily attributed to its rich composition of phenolic compounds, essential oils, vitamin C, carotenoids, and iridoids [2, 4].

Analytical techniques such as high-performance liquid chromatography (HPLC) [5, 6], Gas chromatography (GC) [7], spectrophotometry [8], and refractometry [9] have been specifically developed for the qualitative and quantitative determination of individual phytoconstituents of Gilaburu rather than for its total composition. However, both GC and HPLC have certain drawbacks, including the requirement for expensive instrumentation, time-consuming and labor-intensive procedures, the need for qualified personnel, the inapplicability of GC to thermolabile compounds, and the generation of large volumes of toxic and environmentally hazardous solvent waste in HPLC [10].

Spectroscopic techniques are limited by high instrumentation costs, large sample requirements, complex chemical preparation, the need for trained personnel, and sensitivity to environmental factors such as pH, temperature, and impurities [11]. In contrast to conventional techniques, electrochemical methods offer key advantages such as high sensitivity, low detection limits, rapid response, minimal sample requirements, simple protocols, cost-effective instrumentation, and compatibility with portable systems [12].

The interaction between various molecules and DNA is critical in drug development, as it reveals potential mechanisms of action and helps enhance efficacy, selectivity, and reduce off-target effects [13]. These interactions may be covalent or non-covalent, with small molecules binding via intercalation, groove binding, or electrostatic forces, thereby affecting gene expression and cellular function. [14]. Among these mechanisms, intercalation is the most prominent, involving the insertion of molecules between DNA base pairs without covalent bonding or disruption of hydrogen bonds. This interaction stabilizes the helix while inducing elongation, increased rigidity, and partial unwinding. Minor groove binding entails hydrogen bonding and close contact with the groove

wall, whereas major groove binding may lead to DNA triplex formation.

Electrostatic interactions, though relatively weak, occur between positively charged molecular regions and the negatively charged phosphate backbone of DNA [15]. Several techniques are utilized to investigate drug-DNA interactions, including spectroscopic methods such as UV-Visible, and fluorescence spectroscopy [16], as well as HPLC [17] and surface plasmon resonance [18]. Due to the limitations of conventional analytical techniques and the distinct advantages of electrochemical methods—such as high sensitivity, low sample volume, and operational simplicity—electrochemical approaches have become a widely preferred strategy for investigating interactions between drug candidates and DNA.

This study is the first to directly characterize the electrochemical properties of Gilaburu extract from its commercial tablet form and to investigate its interaction with double-stranded DNA (dsDNA) using electrochemical techniques. Despite its traditional use and widespread availability as a dietary supplement, the potential interaction of Gilaburu with DNA has not been previously explored. Initially, the electrochemical behavior of the extract was examined, and the effects of pH and scan rate on its redox processes were systematically evaluated.

Then, interaction of Gilaburu extract with dsDNA were carried out in solution phase, and changes in the oxidation peak potentials and currents of guanine and adenine were monitored. The toxicity (S) of the extract toward DNA was determined based on the changes in adenine oxidation peak current.

In this context, the developed electrochemical method enabled rapid AND cost-effective characterization of the redox behavior and DNA-binding interactions of the herbal drug candidate, potentially linked to its pharmacological effects. Elucidating its DNA-targeted mechanisms is crucial for supporting current uses and identifying new therapeutic applications. Direct analysis from tablet form also highlights the method's suitability for quality control.

2. MATERIALS AND METHODS

2.1 Instrumentation

DPV and CV analyses were carried out using an AUTOLAB potentiostat/galvanostat/impedance analyzer.

The AUTOLAB was interfaced with a personal computer via a USB connection and controlled through Nova software. A conventional three-electrode system was employed, comprising a pencil graphite electrode (PGE) as the working electrode,

an Ag/AgCl electrode as the reference, and a platinum wire as the auxiliary electrode. To vortex, DLAB MX-S was employed.

2.2 Chemicals

Glacial acetic acid (CH_3COOH) was obtained from Isolab Chemicals. Boric acid (H_3BO_3), sodium hydroxide (NaOH), sodium chloride (NaCl), dipotassium hydrogen phosphate (K_2HPO_4), and potassium dihydrogen phosphate (KH_2PO_4) were supplied by Merck. dsDNA derived from fish sperm, EDTA disodium salt, and Tris-HCl were purchased from Sigma-Aldrich. All solutions were prepared using ultrapure water (UPW). Buffer solutions comprising 0.5 M acetate (ACB) at pH 3.8, 4.8, and 5.6; 0.05 M phosphate at pH 7.4; and 0.1 M borate at pH 9.8 — each supplemented with 0.02 M NaCl — were utilized, along with 0.05 M Tris-EDTA (TE) buffer at pH 8.0.

Commercial Gilaburine tablets (NHP İlaç Sanayi ve Ticaret AŞ) containing Gilaburu extract were used.

2.3 Electrochemical Characterization of Gilaburu

The tablets containing Gilaburu extract were pulverized, and a Gilaburu stock solution was prepared using UPW. This stock solution was then diluted to the desired concentrations using ACB. Subsequently, the resulting solution was transferred to the electrochemical measurement cell for CV and DPV analyses to determine the electrochemical redox behaviour. Prior to each measurement, PGEs were activated by applying a potential of +1.4 V for 30 s in ACB (pH 4.8) [19].

2.4 Interaction of Gilaburu and DNA

Various concentrations of Gilaburu and a 1000 µg/mL of stock DNA solution were mixed in a 1:1 ratio using ACB. Then, 100 µL of each mixture was transferred into vials and incubated in a thermal shaker at 37 °C and 650 rpm for 1 h. At the end of the incubation, the electrodes were rinsed once with ACB. DPV measurements were subsequently performed in ACB at pH 4.8 [20].

2.5 Measurement

DPV measurements were performed at a scan rate of 100 mV/s with 0.5 s interval time in ACB (pH:4.8) (step potential: 8 mV, modulation amplitude: 80 mV). CV measurements were performed at a scan rate of 50 mV/s with 0.05 s interval time.

3. RESULTS and DISCUSSION

3.1 Electrochemical Profiling of Gilaburu Extract: Redox Behavior and DNA Binding Investigation

To determine the redox peak potentials of Gilaburu extract, DPV measurements were conducted in both anodic and cathodic directions using its ACB-based solution.

Fig.1 shows the resulting voltammograms. ACB was also used as the blank.

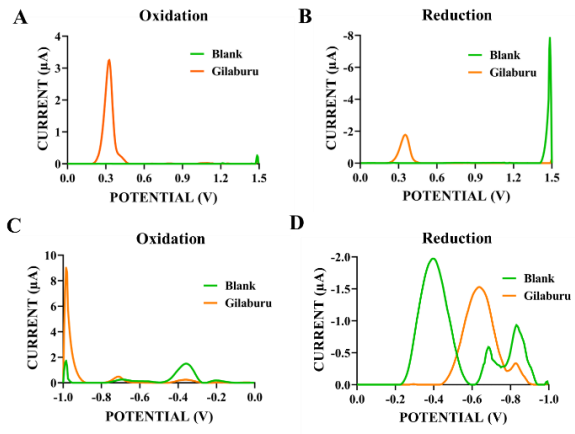

Figure 1: DPV of Gilaburu extract and blank (ACB) in the ranges of oxidation (0 to 1.5 V) **(A)** and reduction (1.5 to 0 V) **(B)**. DPV of Gilaburu extract and blank (ACB) in the ranges of oxidation (-1.0 to 0 V) **(C)** and reduction (0 to -1.0 V) **(D)**.

As shown in Fig.1A, the forward scan from 0 to +1.5 V revealed that the electroactive species in the Gilaburu extract exhibited a prominent oxidation peak current around +0.3 V. In the reverse scan from 1.5 V to 0 V, as presented in Fig.1B, the Gilaburu extract was found to display a reduction peak current at approximately +0.35 V, indicating the presence of reducible components. As shown in Fig.1C, the forward scan from –1.0 V to 0 V (oxidation direction) revealed that the Gilaburu extract did not exhibit any oxidation peak current distinct from those of the blank. In the reverse scan from 0 to –1.0 V, the electroactive species in the Gilaburu extract showed a reduction peak current at approximately –0.6 V. However, the blank also exhibited a major reduction peak around –0.4 V and minor peaks near –0.7 V and –0.8 V (Fig.1D). Upon evaluation of all redox signals of the Gilaburu extract, the oxidation peak current observed around +0.3 V in the anodic scan (0 to +1.5 V) was selected as the target signal for subsequent electrochemical analyses. This potential was preferred since it provided the highest average oxidation peak current (~3 µA), and no interfering redox peaks were detected in the blank within this potential window.

Following the determination of the redox peak potentials of the Gilaburu extract and the selection of the most suitable peak potential for further analysis, detailed characterization and optimization studies were conducted. These experiments aimed to assess the effects of pH and scan rate on the electrochemical behavior of Gilaburu extract. Fig.2 presents DPV and CV data recorded under varying conditions, highlighting changes in the anodic signal near +0.3 V. The figure also includes plots illustrating quantitative relationships derived from the voltammogram.

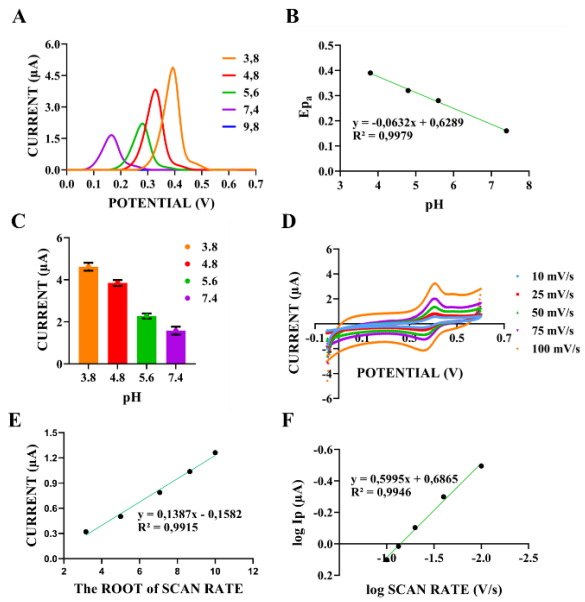

Figure 2: (A) DPV of Gilaburu extract from different supporting electrolytes ranging from pH 3.8 to pH 9.8. **(B)** Correlation plot between the anodic peak potential of the Gilaburu extract and the pH of the supporting electrolyte. **(C)** Histogram illustrating the relationship between the anodic peak current of the Gilaburu extract and the pH of the supporting electrolyte. **(D)** CV of Gilaburu extract at different scan rates ranging from 10 to 100 mV/s with 0.05 s interval time. The plots of the relationships of the anodic peak current of Gilaburu extract vs the square root of the scan rate **(E)**, and the logarithm of the anodic peak current of Gilaburu extract vs the logarithm of the scan rate **(F)** (n=5).

As shown in Fig.2A and 2B, the anodic peak potential of the Gilaburu extract shifts toward more negative values with increasing pH of the supporting electrolyte, indicating that protons are involved in the oxidation of its electroactive constituents [21]. Based on the linear relationship between the anodic peak potential of the Gilaburu extract and the pH of the supporting electrolyte, the following equation was obtained:

E_{pa} = -0.0632 pH + 0.6289 R^2 = 0.9979 **(Equation 1)**

The slope of the equation, determined to be 63.2 mV per pH unit, is very close to the expected theoretical value of 59 mV/pH [22]. This suggests that the electrochemical oxidation of the electroactive constituents in the Gilaburu extract involves an equal number of protons and electrons, as also supported by previous studies [23]. Given that the highest oxidation peak current was observed with the ACB at pH 3.8, this buffer solution was selected for the preparation of the Gilaburu extract solution in the subsequent experiments (Fig. 2C).

Following the evaluation of the effect of pH on the anodic peak potential and current of the Gilaburu extract, the influence of scan rate on its electrochemical behavior was investigated. As illustrated in Fig. 2D, the oxidation current obtained from the Gilaburu extract increases with increasing scan rate (10 to 100 mV/s) in CV measurements. However, as also seen in the figure, no significant shift is observed in the anodic peak potential with increasing scan rate. Based on the data derived from the cyclic voltammogram in Fig.2D, a linear relationship between the square root of the scan rate and the anodic peak current was established (Fig.2E). This relationship yielded the following equation:

I_p (μA) = 0.1387$v^{1/2}$ - 0,1582 R^2 = 0,9915 **(Equation 2)**

As shown in Equation 2, the anodic peak current increases proportionally with the square root of the scan rate, exhibiting a high correlation coefficient. This indicates that the redox behavior of the Gilaburu extract is governed by a diffusion-controlled process, where the electrochemical response is determined by the rate of species transport to and from the electrode surface [24].

In order to validate the diffusion-controlled nature of the electrochemical process of the Gilaburu extract, the logarithmic relationship between the scan rate (log V/s) and the anodic peak current (log I_p) was examined, as depicted in Fig.2F. From this linear correlation, the following equation was derived:

log (I_p (μA)) = 0,5995 log(V/s) + 0,6865 R^2 = 0,9946 **(Equation 3)**

As reported in the literature, a slope value of this equation approaching 0.5 is indicative of a diffusion-controlled electron transfer mechanism, whereas a slope near 1.0 is characteristic of an adsorption-controlled process [25]. The slope value of 0.59 obtained from our equation is close to the theoretical value of 0.5, thereby confirming that the electrochemical process of the Gilaburu extract proceeds via a diffusion-controlled mechanism. The anodic peak potential remained constant across varying scan rates.

According to the literature, a linear correlation between the logarithm of the scan rate (log v) and the peak potential (E_p) is indicative of an electrochemically irreversible electron transfer mechanism for the analyte [26]. However, this behavior does not apply to the Gilaburu extract. As shown in Fig.1A and Fig.1B, the voltammograms recorded between 0 and 1.5 V display a well-defined anodic peak around +0.3 V in the forward scan and a corresponding cathodic peak at the same potential in the reverse scan. This symmetric redox response indicates that the electroactive species in the extract undergo a reversible electron transfer process.

Upon evaluating the influence of pH and scan rate on the electrochemical characteristics of the Gilaburu extract, the LOD was established using the optimized electroanalytical method for its quantification in tablet dosage forms. This parameter is particularly critical for the quality control of dietary supplements, where accurate quantification of the active constituents is required. Compared to classical spectrophotometric and chromatographic techniques, the proposed electrochemical approach enables rapid, cost-efficient, and highly sensitive analysis [27]. Therefore, LOD and LOQ serve as

essential analytical performance metrics to validate the method's applicability for routine analysis [28].

Fig.3 presents the voltammetric responses and corresponding calibration plot of Gilaburu extract solutions at varying concentrations, along with the voltammogram and histogram recorded at different time points to evaluate the solution-phase stability of the extract.

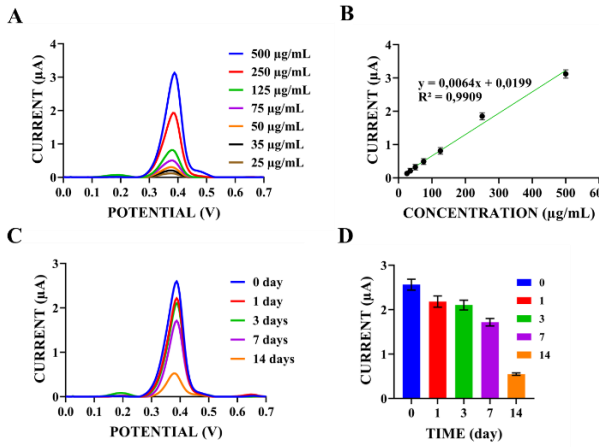

Figure 3: **(A)** DPV of Gilaburu extract recorded in the potential range of 0 to 0.7 V at concentrations ranging from 25 to 500 µg/mL. **(B)** Calibration plot of anodic peak current versus the concentration of Gilaburu extract. **(C)** DPV of Gilaburu extract, stored throughout various day (0-14 days) at 4 °C, recorded in the potential range of 0 to +0.7 V. **(D)** Histogram plot of anodic peak current versus the storage days of solution of Gilaburu extract.

As illustrated in Fig.3A, the anodic peak current exhibits a proportional increase with increasing concentrations of Gilaburu extract in the range of 25–500 µg/mL. In Fig. 3B, a strong linear relationship is observed between the anodic peak current and the extract concentration, with a high correlation coefficient (R^2), indicating excellent linearity. These findings confirm that the developed electrochemical method offers a broad dynamic range (25-500 µg/mL) for the quantitative determination of Gilaburu extract. The limit of detection (LOD) and limit of quantification (LOQ) were determined based on the equations LOD = (3 × sd) / slope and LOQ = (10 × sd) / slope, where sd denotes the standard deviation derived from the regression analysis, corresponding to a signal-to-noise ratio of 3 [29]. According to the aforementioned formulas, LOD, and LOQ for Gilaburu extract in the electrochemical assay were determined as 4.5 µg/mL and 15.1 µg/mL, respectively. Gilaburu extract-containing tablets are commonly formulated with 500 or 1000 mg of active ingredient, and the calculated detection limits demonstrate that even minor deviations in content can be accurately and sensitively identified using the developed electrochemical method, underscoring its applicability for routine quality control analyses.

Electrochemical measurements of the Gilaburu extract in aqueous solution were conducted immediately after preparation, and subsequently at defined intervals during storage at 4 °C to evaluate its temporal stability. As shown in Fig.3C, the anodic peak current gradually decreased

over time, indicating the degradation of electroactive species during storage.

In Fig.3D, the histogram shows that the average anodic peak current decreased by approximately 18% on the third day (2.19 ± 0.25 µA) compared to the initial value (2.56 ± 0.25 µA). By the end of the first week, the average anodic peak current further declined to 1.72 ± 0.17 µA, corresponding to a 33% reduction relative to the initial measurement. A pronounced decrease was observed at the end of the second week, where the average anodic peak current dropped to 0.55 ± 0.03 µA, representing a 79% decrease. These findings clearly demonstrate that the stability of the Gilaburu extract in aqueous medium is substantially compromised over time, indicating limited suitability for long-term storage in solution form.

3.2 Interaction with DNA

The anticancer and antimicrobial properties of Gilaburu extract have been reported in the literature [4]. Considering that these biological activities may be mediated through interactions with DNA, the potential molecular mechanisms were explored by investigating the interaction between Gilaburu extract and dsDNA.

Fig. 4 shows the voltammograms and corresponding histogram depicting the changes in the oxidation peak currents of guanine and adenine upon interaction of a fixed dsDNA concentration with varying concentrations of Gilaburu extract in solution phase.

The histogram specifically highlights the variation in adenine oxidation peak currents as a function of Gilaburu extract concentration.

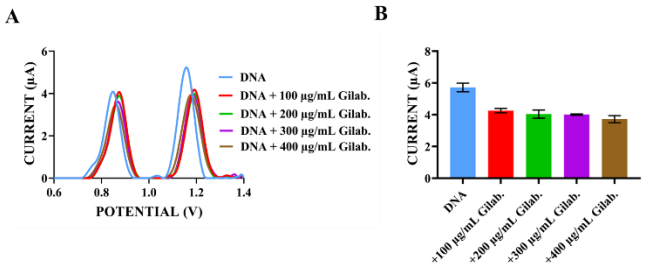

Figure 4: (A) DPV after the interaction between different concentrations (100-400 µg/mL) of Gilaburu extract and dsDNA, taken in ACB (pH:4.8) within the potential range of 0.6 V to 1.4 V. **(B)** Histogram presenting the change in the average adenine anodic current as a result of the interaction between different concentrations (25-125 µg/mL) of Gilaburu extract and dsDNA.

As shown in Fig.4A, DPV was performed in acetate buffer (pH 4.8) following the interaction of dsDNA (500 µg/mL) with increasing concentrations (100–400 µg/mL) of Gilaburu extract. The voltammogram reveals the effects on the anodic peak potentials and currents of guanine and adenine bases. While guanine oxidation current remained largely unchanged at 100 and 200 µg/mL extract, it gradually decreased at higher concentrations—dropping to 3.77 ± 0.16 µA at 300 µg/mL and to 3.22 ± 0.48 µA at 400 µg/mL, indicating a

~21% reduction relative to the initial value (4.08 ± 0.32 µA).

These results suggest that Gilaburu extract has a limited impact on the electrochemical oxidation of guanine residues in dsDNA. However, as demonstrated in Fig.4A and the corresponding histogram in Fig.4B, adenine exhibited a more substantial attenuation in its electrochemical response compared to guanine, indicating a stronger interaction or higher susceptibility to signal suppression upon exposure to the extract. Prior to the interaction, the average anodic peak current of adenine was measured as 5.72 ± 0.54 µA. Following incubation with 100 µg/mL of Gilaburu extract, the current decreased to 4.26 ± 0.28 µA (approximately 26% reduction), and further declined to 4.04 ± 0.52 µA (≈29% reduction) with 200 µg/mL extract, 3.96 ± 0.04 µA (≈31% reduction) with 300 µg/mL, and ultimately to 3.72 ± 0.26 µA (≈35% reduction) with 400 µg/mL extract. The results reveal a gradual, dose-dependent interaction of Gilaburu extract with dsDNA, indicative of a partial and concentration-related electrochemical response. Prior to the interaction, the anodic peak potential of adenine was observed around +1.15 V, whereas after interaction with Gilaburu extract, it shifted to approximately +1.19 V. According to the literature, such a positive shift in peak potential following interaction with DNA suggests that the binding of Gilaburu extract to dsDNA may occur via an intercalative mechanism [30].

Based on anodic peak currents of adenine, Gilaburu extracts toxicity effect (S) on dsDNA was calculated according to the following equation :

$S = (S_a/S_b) \times 100$ **(Equation 4)**

S: Percentage of the adenine peak current change

S_a: The magnitude of the adenine current after interaction

S_b: The magnitude of the adenine current before interaction

Typically, S values greater than 85 denote a non-toxic profile, whereas values in the 50–85 range reflect moderate toxicity. S values under 50 are interpreted as toxic [31]. Using this equation, the S value of Gilaburu extract on dsDNA was calculated as 65.03%, implying a moderate level of toxicity towards dsDNA. The calculated value corroborates our findings, verifying that Gilaburu extract exerts a partial influence on dsDNA, indicative of a moderate interaction.

4. CONCLUSION

In the study, electrochemical characterization and detection of Gilaburu extract from pharmaceutical formulation and its interaction with DNA were examined for the first time. It was determined that the Gilaburu extract

exhibits multiple anodic and cathodic redox peak potentials suitable for its direct electrochemical detection, with the most pronounced anodic peak current observed at approximately +0.3 V. The electrochemical processes of the redox-active species in the extract were found to be diffusion-controlled, and it was revealed that an equal number of protons and electrons participate in these redox reactions upon the involvement of protons in the process. Additionally, potential scans in both the forward and reverse directions indicated that the system exhibits a reversible electrochemical behavior. By employing the developed electrochemical method for direct analysis of tablet formulations, Gilaburu extract was quantitatively determined within a broad linear concentration range of 25–500 µg/mL, with LOD and LOQ values of 4.5 µg/mL and 15.1 µg/mL, respectively. The capability to detect very low concentrations of active ingredients from pharmaceutical and nutraceutical formulations—as demonstrated in this study—with high sensitivity and in a rapid, cost-efficient manner compared to conventional techniques, is of great importance for drug development and formulation studies. In order to gain insight into the previously reported anticancer and antimicrobial properties of Gilaburu extract, its interaction with DNA was investigated for the first time. Solution-phase studies demonstrated that the extract exerts a dose-dependent partial effect on DNA. Upon interaction, the oxidation peak potential of adenine bases in DNA shifted toward more positive values, suggesting that the interaction may occur via intercalation of the extract's constituents into the DNA double helix. The toxicity of Gilaburu extract on DNA was quantitatively evaluated and found to be approximately 65%, indicating a moderate level of DNA-associated toxicity. These findings indicate that the interaction of Gilaburu extract with DNA may contribute to its overall pharmacological activity, particularly in relation to its bioactive properties.

5. Funding

This research was funded by TÜBİTAK, 2209-A University Students (Undergraduate Students) Research Projects Support Program, Project Number of 1919B012301367.

6. Ethics approval and consent to participate

This study does not need any Ethics report.

7. Consent for publication

The Authors give consent for publication.

8. Availability of data and materials

All data and materials of the paper are available to the public.

9. Authors' contributions

Hüseyin Oğuzhan KAYA: Writing – original draft, Writing – review & editing, Investigation, Conceptualization, Methodology, Formal analysis.

Sena ALACACI: Investigation, Methodology, Funding acquisition.

Seda Nur TOPKAYA: Writing – original draft, Writing – review & editing Investigation, Conceptualization, Methodology, Formal Analysis, Validation, Funding acquisition, Supervision.

Disclosure statement

No potential conflict of interest was reported by the author(s).

REFERENCES

1. Dhama K, Karthik K, Khandia R, et al (2018) Medicinal and Therapeutic Potential of Herbs and Plant Metabolites / Extracts Countering Viral Pathogens - Current Knowledge and Future Prospects. Curr Drug Metab 19:236–263. https://doi.org/10.2174/1389200219666180129145252
2. GÜLEŞCİ N (2019) Viburnum Opulus L. (Adoxaceae) Meyvesinin Antimikrobiyal, Antioksidan ve Kimyasal İçeriği Yönünden Metabolizmaya Etkilerinin Değerlendirilmesi Üzerine Bir Derleme. İstanbul Gelişim Üniversitesi Sağlık Bilimleri Dergisi 920–928. https://doi.org/10.38079/igusabder.594480
3. Kajszczak D, Zakłos-Szyda M, Podsędek A (2020) Viburnum opulus L.—A Review of Phytochemistry and Biological Effects. Nutrients 12:3398. https://doi.org/10.3390/nu12113398
4. Şahin B, Bülbül AS, Çelik IS, et al (2021) Investigation of biological activities of plant extract and green synthesis silver nanoparticles obtained from Gilaburu (Viburnum opulus L.) fruits. Turk J Chem 46:224–235. https://doi.org/10.3906/kim-2108-48
5. Özrenk K, Gündoğdu M, Keskin N, Kaya T (2011) Some Physical and Chemical Characteristics of Gilaburu (Viburnum opulus L.) Fruits in Erzincan Region. Iğdır Univ J Inst Sci & Tech 4:9–14
6. M. Levent; SEVER YILMAZ A (2007) Viburnum opulus L. ve Viburnum lantana L.'da amentoflavon HPLC analizi. Ankara Universitesi Eczacilik Fakultesi Dergisi 36:161–169. https://doi.org/10.1501/Eczfak_0000000531
7. Adebayo AH, Alade AB, Yakubu OF (2017) Gas chromatography-mass spectrometry analysis of viburnum opulus (L) extract and its toxicity studies in rats. Asian Journal of Pharmaceutical and Clinical Research 10:383–388. https://doi.org/10.22159/AJPCR.2017.V10I6.17350
8. Česonienė L, Daubaras R, Viškelis P, Šarkinas A (2012) Determination of the Total Phenolic and Anthocyanin Contents and Antimicrobial Activity of Viburnum Opulus Fruit Juice. Plant Foods for Human Nutrition 67:256–261. https://doi.org/10.1007/S11130-012-0303-3
9. Polat M, Mertoğlu K, Eskimez İ (2021) Physico-Chemical Characteristics of Some Gilaburu (Viburnum Opulus L.) Genotypes. International Journal of Agriculture Environment and Food Sciences 5:51–55. https://doi.org/10.31015/JAEFS.2021.1.7

10. Xie Z, Koysomboon C, Zhang H, et al (2022) Vinegar Volatile Organic Compounds: Analytical Methods, Constituents, and Formation Processes. Front Microbiol 13:. https://doi.org/10.3389/fmicb.2022.907883

11. Zaukuu J-LZ, Benes E, Bázár G, et al (2022) Agricultural Potentials of Molecular Spectroscopy and Advances for Food Authentication: An Overview. Processes 10:214. https://doi.org/10.3390/pr10020214

12. Baranwal J, Barse B, Gatto G, et al (2022) Electrochemical Sensors and Their Applications: A Review. Chemosensors 10:363. https://doi.org/10.3390/chemosensors10090363

13. Selvaraj C, Singh SK (2019) Computational and Experimental Binding Mechanism of DNA-drug Interactions. Curr Pharm Des 24:3739–3757. https://doi.org/10.2174/1381612824666181106101448

14. Rauf S, Gooding JJ, Akhtar K, et al (2005) Electrochemical approach of anticancer drugs–DNA interaction. J Pharm Biomed Anal 37:205–217. https://doi.org/10.1016/j.jpba.2004.10.037

15. Shahabadi N, Fili SM, Kheirdoosh F (2013) Study on the interaction of the drug mesalamine with calf thymus DNA using molecular docking and spectroscopic techniques. J Photochem Photobiol B 128:20–26. https://doi.org/10.1016/j.jphotobiol.2013.08.005

16. Oguzcan E, Koksal Z, Taskin-Tok T, et al (2022) Spectroscopic and molecular modeling methods to investigate the interaction between psycho-stimulant modafinil and calf thymus DNA using ethidium bromide as a fluorescence probe. Spectrochim Acta A Mol Biomol Spectrosc 270:120787. https://doi.org/10.1016/j.saa.2021.120787

17. Kuzpınar E, Al Faysal A, Şenel P, et al (2024) Quantification of mirtazapine in tablets via DNA binding mechanism; development of a new HPLC method. Journal of Chromatography B 1234:124019. https://doi.org/10.1016/j.jchromb.2024.124019

18. Johari-Ahar M, Abdian M, Maleki S, et al (2023) Intercalation of anticancer drug mitoxantrone into DNA: Studied by spectral and surface plasmon resonance methods. J Mol Struct 1274:134509. https://doi.org/10.1016/j.molstruc.2022.134509

19. Kaya HO, Bozdemir C, İstanbullu H, Topkaya SN (2025) Probing Redox Responses and DNA Interactions in Drug Discovery. Drugs and Drug Candidates 4:20. https://doi.org/10.3390/ddc4020020

20. Kaya HO, Albayrak G, Isbilir H, et al (2024) Electrochemical profiling of natural furanocoumarins: DNA interaction dynamics of oxypeucedanin and prantschimgin. ADMET DMPK 12:319–334. https://doi.org/10.5599/admet.2199

21. Aftab S, Kurbanoglu S, Ozcelikay G, et al (2019) Carbon quantum dots co-catalyzed with multiwalled carbon nanotubes and silver nanoparticles modified nanosensor for the electrochemical assay of anti-HIV drug Rilpivirine. Sens Actuators B Chem 285:571–583. https://doi.org/10.1016/j.snb.2019.01.094

22. Kaya SI, Demirkan B, Bakirhan NK, et al (2019) Highly sensitive carbon-based nanohybrid sensor platform for determination of 5-hydroxytryptamine receptor agonist (Eletriptan). J Pharm Biomed Anal 174:206–213. https://doi.org/10.1016/j.jpba.2019.05.070

23. Samanci SN, Ozcelikay-Akyildiz G, Atici EB, Ozkan SA (2025) Electrochemical behaviour and determination of niraparib using glassy carbon and boron-doped diamond electrodes. Diam Relat Mater 152:111964. https://doi.org/10.1016/j.diamond.2025.111964

24. Mohamed MA, El-Gendy DM, Ahmed N, et al (2018) 3D spongy graphene-modified screen-printed sensors for the voltammetric determination of the narcotic drug codeine. Biosens Bioelectron 101:90–95. https://doi.org/10.1016/j.bios.2017.10.020

25. Samanci SN, Ozcelikay-Akyildiz G, Atici EB, Ozkan SA (2025) Electrochemical behaviour and determination of niraparib using glassy carbon and boron-doped diamond electrodes. Diam Relat Mater 152:111964. https://doi.org/10.1016/j.diamond.2025.111964

26. Aydogdu Ozdogan N, Demir E, Ozkan SA (2025) Development of a New Generation MWCNT/TiO_2/TiO_2-Based Voltammetric Sensors for the Detection of Daptomycin in Soil and Different Water Samples. ChemElectroChem e202400675. https://doi.org/10.1002/celc.202400675

27. Bitew Z, Amare M (2020) Recent reports on electrochemical determination of selected antibiotics in pharmaceutical formulations: A mini review. Electrochem commun 121:106863. https://doi.org/10.1016/j.elecom.2020.106863

28. Pandelova A, Stoyanov N, Dzhudzhev B (2023) Determination of Limit of Detection in Electrochemical Biosensors. In: 2023 International Scientific Conference on Computer Science (COMSCI). IEEE, pp 1–4

29. Soyler D, Dolgun V, Kurbanoglu S, et al (2025) Synthesis and design of functional fullerenol-based electrochemical nanobiosensor to examine the inhibition effects of anti-Alzheimer drug active pyridostigmine on acetylcholinesterase. Measurement 253:117494. https://doi.org/10.1016/j.measurement.2025.117494

30. Bilge S, Dogan Topal B, Caglayan MG, et al (2022) Human hair rich in pyridinic nitrogen-base DNA biosensor for direct electrochemical monitoring of palbociclib-DNA interaction. Bioelectrochemistry 148:108264. https://doi.org/10.1016/j.bioelechem.2022.108264

31. Muti M, Muti M (2018) Electrochemical monitoring of the interaction between anticancer drug and DNA in the presence of antioxidant. Talanta 178:1033–1039. https://doi.org/10.1016/j.talanta.2017.08.089